Carbohydrate Polymers 116 (2015) 223–228

Contents lists available at ScienceDirect

Carbohydrate Polymers

journal homepage: www.elsevier.com/locate/carbpol

Nanocellulose-alginate hydrogel for cell encapsulation

Minsung Park[a], Dajung Lee[a], Jinho Hyun[a,b,*]

[a] Department of Biosystems and Biomaterials Science and Engineering, Seoul National University, Seoul 151-921, Republic of Korea
[b] Research Institute for Agriculture and Life Sciences, Seoul National University, Seoul 151-921, Republic of Korea

ARTICLE INFO

Article history:
Received 2 December 2013
Received in revised form 10 July 2014
Accepted 27 July 2014
Available online 4 August 2014

Keywords:
TEMPO-oxidization
Bacterial cellulose
Alginate
Cell encapsulation

ABSTRACT

TEMPO-oxidized bacterial cellulose (TOBC)-sodium alginate (SA) composites were prepared to improve the properties of hydrogel for cell encapsulation. TOBC fibers were obtained using a TEMPO/NaBr/NaClO system at pH 10 and room temperature. The fibrillated TOBCs mixed with SA were cross-linked in the presence of Ca^{2+} solution to form hydrogel composites. The compression strength and chemical stability of the TOBC/SA composites were increased compared with the SA hydrogel, which indicated that TOBC performed an important function in enhancing the structural, mechanical and chemical stability of the composites. Cells were successfully encapsulated in the TOBC/SA composites, and the viability of cells was investigated. TOBC/SA composites can be a potential candidate for cell encapsulation engineering.

1. Introduction

Cell encapsulation has garnered attention as a technology to provide immunoprotection for transplanted cells. The cells can be protected from the immune systems by a semipermeable membrane that allows nutrients and secreted proteins to permeate while isolating the cells from hostile immune reactions. Therefore, the transplantation of encapsulated cells has been suggested as a promising cell-based treatment for a variety of diseases, such as diabetes, metabolic deficiencies, liver failure, cancer, and neurodegenerative and cardiovascular diseases (Orive et al., 2003; Rokstad, Lacik, de Vos, & Strand, 2014; Schmidt, Rowley, & Kong, 2008; Zhang et al., 2013).

Alginate is a biopolymer that forms a hydrogel in the presence of divalent cations, such as Ca^{2+} (Draget, Steinsvag, Onsoyen, & Smidsrod, 1998). Because alginate hydrogels have excellent biocompatibility, they have been preferentially used to protect transplanted cells from immune rejection and as a matrix to increase the cell viability in cell encapsulation (Bratlie, York, Invernale, Langer, & Anderson, 2012; Orive, Tam, Pedraz, & Halle, 2006; Tam et al., 2011; Rokstad et al., 2014). However, the mechanical and chemical stability of alginate is not sufficient to achieve long-term transplantation. Consequently, reinforcing materials need to be added to an alginate matrix to overcome this limitation (Chan et al., 2011; Cordoba, Deladino, & Martino, 2013; Santagapita, Mazzobre, & Buera, 2012).

Bacterial cellulose (BC) biosynthesized by *Gluconacetobacter xylinus* has a high aspect ratio of high crystalline nanofibers (Klemm, Heublein, Fink, & Bohn, 2005; Park, Cheng, Choi, Kim, & Hyun, 2013b; Watanabe, Tabuchi, Morinaga, & Yoshinaga, 1998). BC nanofibers show better mechanical properties and higher hydrophilicity than celluloses from other sources (Hu, Chen, Yang, Liu, & Wang, 2011; Park, Chang, Jeong, & Hyun, 2013a). In spite of its promising properties, BC nanofibers cannot be easily applied as a component of composites due to their inter-connected 3D structure based on a large number of hydrogen bonds. Recently, a 2,6,6-tetramethylpiperidine-1-oxyl radical (TEMPO)-oxidation process was developed to modify the surface of cellulose, and well dispersed cellulose fibrils could be effectively obtained using the electrostatic repulsion of fibers under mild and environmentally friendly conditions compared to other methods (Isogai, Saito, & Fukuzumi, 2011; Saito, 2010).

In this study, TEMPO-mediated oxidized bacterial cellulose (TOBC) was used to improve the mechanical and chemical stability of an alginate hydrogel. TOBC and alginate have a similar chemical structure, and they both participate in the Ca^{2+} crosslinking process. The carboxyl groups on the surface of TOBC provided the possibility of participating in the construction of an alginate-based composite and played important roles in the structural, mechanical and chemical stability. The viability of cells encapsulated in the TOBC-alginate composite was investigated for possible biomedical application of the composite in the future.

* Corresponding author at: Seoul National University, Department of Biosystems and Biomaterials Science and Engineering, 1 Gwanakro Gwanakgu, Seoul 151-921, Republic of Korea. Tel.: +82 28804624; fax: +82 28732285.
E-mail address: jhyun@snu.ac.kr (J. Hyun).

http://dx.doi.org/10.1016/j.carbpol.2014.07.059
0144-8617/

2. Experimental

2.1. Biosynthesis and purification of BC

G. xylinus (KCCM 40216) was obtained from the Korean Culture Center of Microorganisms. The bacterium was cultured on mannitol medium containing 2.5% (w/w) mannitol, 0.5% (w/w) yeast extract and 0.3% (w/w) bacto-peptone. Bacteria were introduced into Petri dishes containing culture medium at 28 °C for 5 days. After incubation, the BC membrane biosynthesized on the surface of the liquid culture medium was harvested and purified with 1 wt% NaOH (SAMCHUN Chemical, Korea) followed by washing with distilled water. This step was repeated to remove the medium components and bacteria. The membrane was stored in distilled water prior to use.

2.2. Preparation of the TEMPO-oxidized BC

The BC was oxidized using a TEMPO (Sigma-Aldrich, USA)-mediated system. To obtain the TEMPO-oxidized BC, 20 g of hydrogel (wet weight) was cut into small pieces and suspended in 500 mL of distilled water containing 20 mg TEMPO and 0.5 g NaBr (Sigma-Aldrich, USA). Subsequently, 15 mL NaClO (Sigma-Aldrich, USA) solution was added to the BC suspension to initiate the oxidation. The system was maintained at pH10 with NaOH. The mixture was vigorously agitated using a magnetic stirrer for 2 days. The oxidation was quenched by adding ethanol (SAMCHUN Chemical, Korea) to the suspension at the end of the reaction. The products were washed with deionized water, collected by centrifugation three times, and then freeze-dried for further experiments.

2.3. Preparation of SA/TOBC beads

The extrusion technique was used to prepare the alginate/TOBC beads. Briefly, 1 mL syringes (Korea Vaccine Co., Ltd., Korea) were filled with sodium alginate (Sigma-Aldrich, USA) solutions containing various amounts of TOBC. The solutions were extruded using syringe pump (US/KDS 100, KD Scientific, USA) and dropped into a calcium chloride (2%) bath aerated with N_2 for gelation. The total concentration of each sample was 20 mg/mL. Thus, 200 mg sodium alginate (SA), 180 mg sodium alginate and 20 mg TOBC (SA/TOBC10), or 160 mg sodium alginate and 40 mg of TOBC (SA/TOBC20) were dissolved in 10 mL of distilled water. To encapsulate the cells, 2 mL of a fibroblast cell (NIH3T3, obtained from KCLB) suspension was mixed with 2 mL of autoclaved (121 °C, 20 min) sodium alginate solution containing various amounts of TOBC. One milliliter of the cell suspension/polymer mixture was extruded through a syringe pump and dropped into a calcium chloride (2%) bath aerated with N_2 gas for gelation. The encapsulated cells were transferred to Petri dishes immediately after the gelation and stored in phosphate buffered saline (PBS, Gibco, USA) prior to use.

2.4. Characterization of SA/TOBC beads

The electron transmission images of SA/TOBC beads containing encapsulated cells were captured by energy-filtering transmission electron microscopy (EF-TEM, LIBRA 120, Carl Zeiss, Germany) at an acceleration voltage of 200 kV. The morphology of the samples was observed at an acceleration voltage of 2 kV using field emission scanning electron microscopy (FE-SEM, SUPRA 55VP, Carl Zeiss, Germany). The chemical structures of the samples were characterized by Fourier transform infrared spectroscopy (FT-IR spectroscopy, Nicolet iS5, Thermo Scientific, USA), and the crystal structure of the samples was determined using a high-resolution X-ray diffractometer (XRD, D8 DISCOVER, Bruker, Germany). The mechanical properties of SA/TOBC beads (compression test) were investigated using a Universal testing machine (UTM, GB/LRX Plus, Lloyd, UK) fitted with a 10 N load cell. For compression testing, 2 mm diameter spherical samples were prepared and compressed to 40% of their original thickness with a constant crosshead speed of 2 mm/min at room temperature. The chemical resistance properties and morphological change were observed by soaking the beads in 40 mM sodium citrate (Sigma-Aldrich, USA) solution for 1 h.

Model molecules with different molecular weights were used to evaluate the diffusion properties of SA/TOBC beads, i.e. dextran-conjugated FITC at 4 kDa and 150 kDa *MW* (Sigma-Aldrich, USA). SA/TOBC beads were incubated in 3 mg/mL of the model molecule solutions, and the permeability of the molecules was determined using confocal microscopy (LSM510, Carl Zeiss).

2.5. Proliferation and viability of encapsulated cells

To study the proliferation of cells encapsulated in the beads, the number of cells in each sample was counted as a function of the incubation day. The cells were encapsulated in beads of SA, SA/TOBC10, and SA/TOBC20 using 2 mL of fibroblast cell suspension (2.3×10^6 cells/mL) mixed with 2 mL polymer solutions according to the method mentioned above. After the gelation, the beads were washed with PBS and collected by centrifugation. After collecting the beads, they were re-dispersed in 20 mL of culture medium. One milliliter of cell-containing bead suspension was added to a Petri dish (SPL, 60 mm × 15 mm) with 1 mL of fresh culture medium. The culture medium consisted of Dulbecco's minimal essential medium (DMEM) supplemented with 10% fetal bovine serum (FBS), penicillin (100 U/mL), streptomycin (100 μg/mL), and HEPES (7.5 mM). The cells encapsulated in SA, SA/TOBC10, and SA/TOBC20 beads were cultured in a humidified 5% CO_2 incubator at 37 °C for 1, 3, and 5 days. After incubation, the encapsulated cells in Petri dishes were recovered using 80 mM sodium citrate and 2.5% trypsin (Gibco, USA), followed by centrifugation. The encapsulated cells from three Petri dishes were counted using a hemocytometer (Marienfeld, Germany). To investigate the viability of encapsulated cells, the cells were recovered from the beads using 80 mM sodium citrate and centrifugation. A live/dead viability/cytotoxicity kit was used to test the viability of mammalian cells (Invitrogen, USA). The indicated combined live/dead assay reagents were added to a Petri dish containing recovered cells, and the mixture was then incubated for 1 h at room temperature in the dark. Green (live cells) and red (dead cells) fluorescence images were collected separately using a fluorescence microscope (BX51, Olympus, Japan).

3. Results and discussion

BC was successfully selectively oxidized at the C6 carbon using TEMPO (Fig. 1A). The asymmetric stretching band at 1602 cm^{-1} of the FTIR spectra indicated chains modified by carboxyl groups. Moreover, the stretching vibration band of the C—H at 2896–2990 cm^{-1} and stretching vibration band of the —OH groups near 3345–3539 cm^{-1} were considerably reduced after the modification in TOBC (Dong, Snyder, Williams, & Andzelm, 2013; Fujisawa, Okita, Fukuzumi, Saito, & Isogai, 2011; Lin, Bruzzese, & Dufresne, 2012).

The effect of oxidation on the crystalline structure of BC was further investigated with XRD and TEM analysis. Because the TEMPO-mediated oxidation of BC fibers only occurred at the surface of cellulose fibers, the original morphology, such as the aspect ratio of fibers and the integrity of the crystal, were maintained. As shown in Fig. 1C, TOBC still distinctly presented the diffraction peaks of BC at 2theta angles near 14, 16, and 22 (Lin et al., 2012; Zhang et al., 2010). Fig. 1D–F shows the changes in the morphology

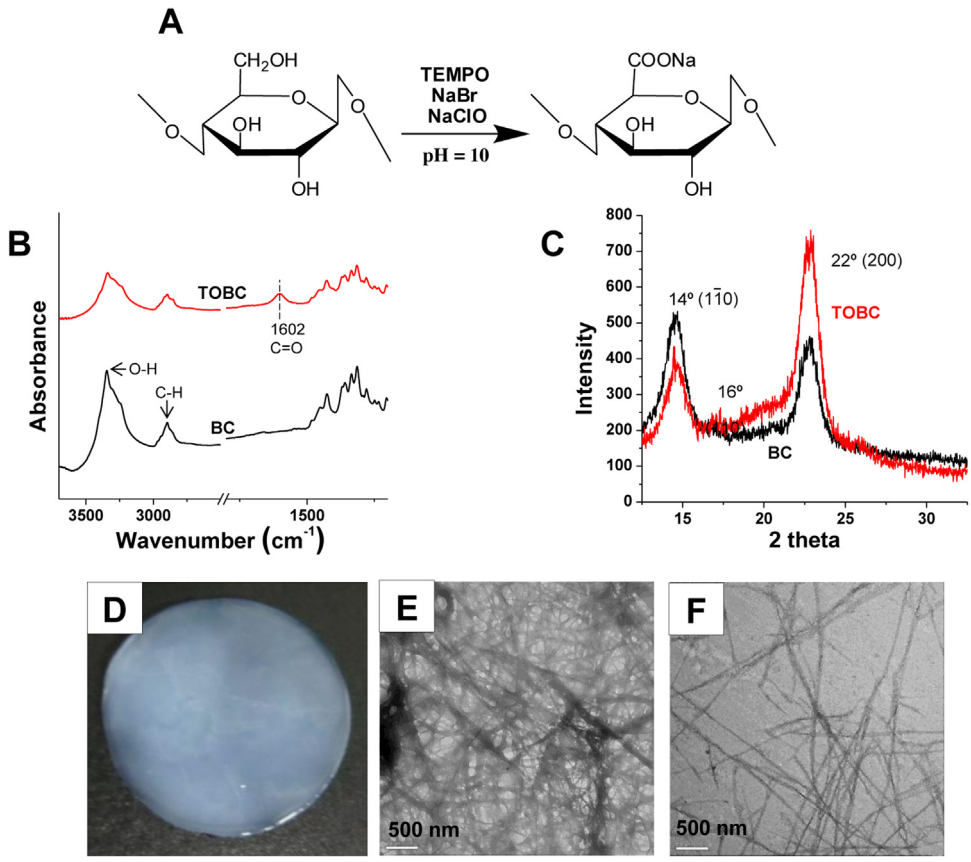

Fig. 1. Preparation of the TEMPO-oxidized BC. Selective oxidation of C6 primary hydroxyls of cellulose to carboxylate groups was performed by TEMPO/NaBr/NaClO oxidation in water at pH = 10. (A) Chemical structure of TOBC. (B) FTIR spectra of pure BC and TOBC. (C) X-ray diffraction patterns of the pure BC and TOBC. (D) Optical image of pure BC. TEM images of (E) pure BC and (F) TEMPO-oxidized BC.

and dimension of BC before and after oxidization. Pure BC exhibited an entangled network structure that was several micrometers in length and tens of nanometers in diameter. Although the fibers slightly shortened, the fiber structure was maintained. The introduction of carboxyl groups at the surface of the BC fibrils increased the gaps between adjacent fibers as a result of the repulsive interaction of anionic charges, which resulted in a well-dispersed state. The TOBC nanofibers with a high aspect ratio were morphologically similar to the BC fibers but showed fewer bundles and networks due to the lack of adhesion between nanofibers.

Although SA showed an amorphous structure, the crystallinity of SA/TOBC composites gradually increased as the cellulose content increased. This relationship was confirmed by the diffraction peaks at 14°, 16°, and 22°, which were characteristic of crystalline cellulose (Fig. 2B). FTIR analysis confirmed the intermolecular interactions between the SA and TOBC components (Fig. 2A). The peak at 1598 cm^{-1} is characteristic of the carbonyl group of SA. As the amount of TOBC added to the alginate increased, the characteristic band shifted toward a higher wavelength. Specifically, a peak located at 1598 cm^{-1} in SA shifted to 1603 cm^{-1} with the addition of TOBC. The shift indicated that the carboxylic groups in TOBC could be attributed to cross-linking network with SA through ionic interactions (Lin et al., 2012).

The compressive mechanical properties of the SA/TOBC composites were evaluated. As expected, the mechanical properties of the composites depended on the TOBC content. The compressive

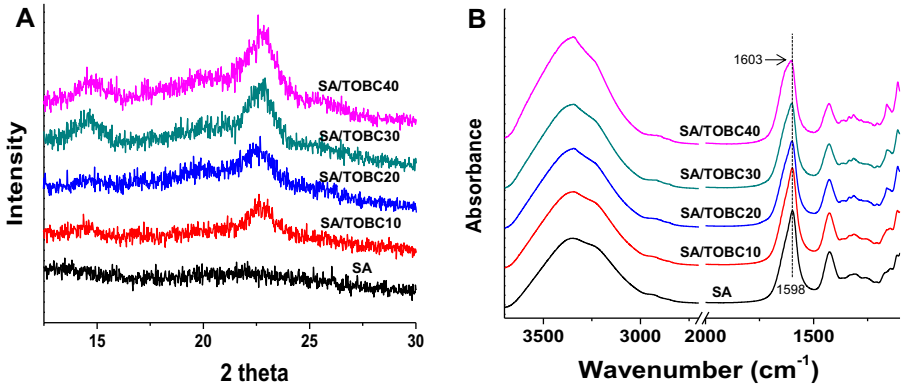

Fig. 2. (A) FTIR spectra for TOBC/SA composites with various cellulose contents. (B) XRD patterns for TOBC/SA composites with various TOBC contents.

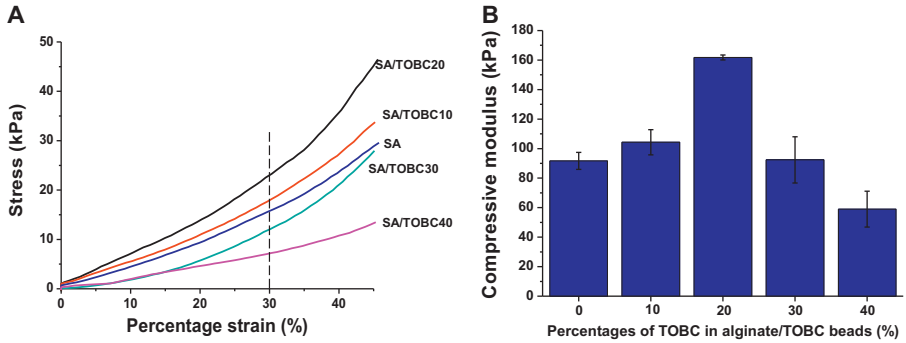

Fig. 3. (A) Compressive stress–strain curves and (B) compressive modulus of TOBC/SA beads.

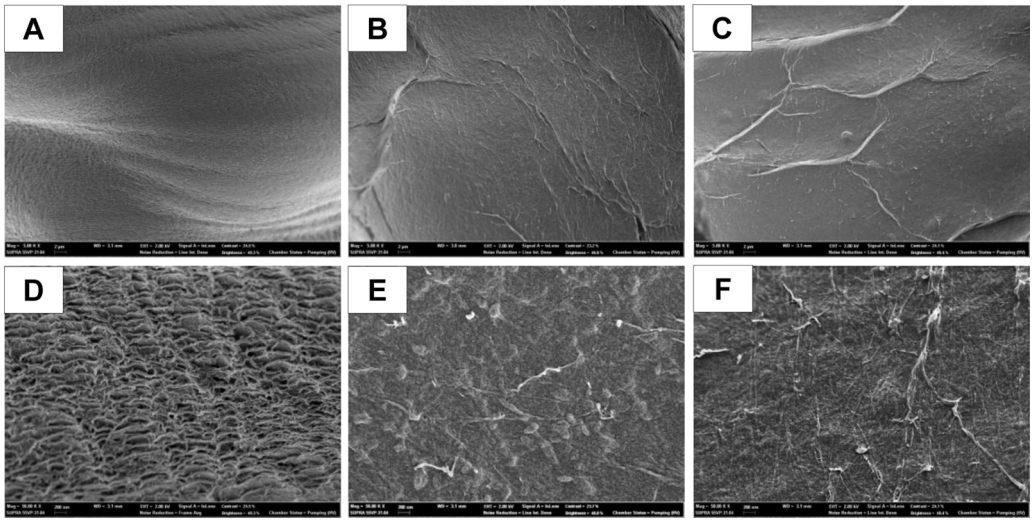

Fig. 4. SEM images of TOBC/SA microbeads. (A) SA beads, (B) SA/TOBC10 beads and (C) SA/TOBC20 beads. ((D)–(F)) are magnified images of ((A)–(C)).

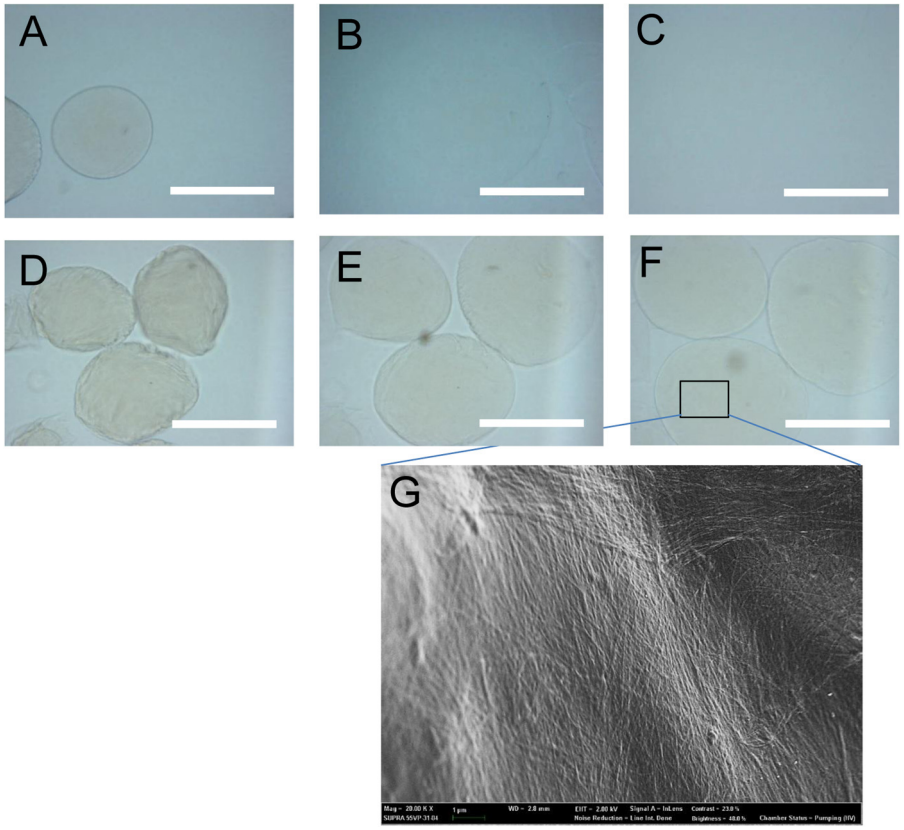

Fig. 5. Microscopic images of SA and SA/TOBC20 microbeads after being exposed to 40 mM sodium citrate for 0 min ((A) and (D)), 5 min ((B) and (E)) and 60 min ((C) and (F)). Scale bar = 500 μm. (G) SEM image of SA/TOBC20 microbead of (F).

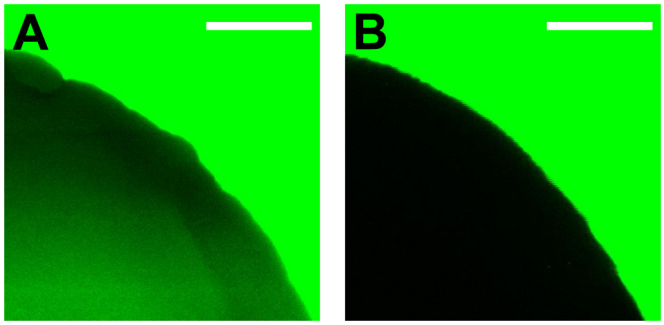

Fig. 6. Confocal microscopy section images for permeability assessment of SA/TOBC20 microbeads incubated with 4 kDa FITC–dextran (A) and 150 kDa FITC–dextran (B). Scale bar = 50 μm.

stress–strain curves showed that the addition of less than 20% of TOBC formed more robust beads than the beads formed with SA only. The compressive modulus of beads also positively correlated with the TOBC content (Fig. 3B). The results showed that introducing TOBC to the SA hydrogel matrix enhanced the mechanical strength of the composites. TOBC could participate in the crosslinking reaction and cooperate well with SA to act as a structural frame. However, the addition of more than 30% of TOBC deteriorated the compressive strength of beads (Fig. 3A) by inducing the slippage of TOBC nanofibers. The TOBC chains not involved in crosslinking weakened the composite. Fig. 4 shows the SEM images of the beads formed with different amounts of TOBC in the SA/TOBC composite. While the surface of SA beads was porous, the surface of SA/TOBC beads became nonporous after TOBC was introduced into SA because the mixture of TOBC nanofibers and SA created a networked structure by coupling with divalent ions.

The chemical stability of the beads was evaluated by soaking them in an aqueous solution of 40 mM sodium citrate for chelating with calcium. The morphological changes of the gel beads were observed after 5 and 60 min (Fig. 5). The SA beads soaked in the solution for 5 min had disintegrated and lost their spherical shape due to drastic swelling caused by the chelation of calcium ions (Fig. 5A and B). Forty millimolar sodium citrate was found to be sufficient to extract most of calcium ions from SA beads. This effect is undesirable in biomedical applications because it would lead to a loss of immunoprotective properties and enhance the host responses in the body. Further exposing the SA beads to the sodium citrate solution for 60 min resulted in their complete dissolution (Fig. 5C). In contrast, the SA/TOBC beads were observed to maintain their spherical shape even after 60 min (Fig. 5D–F). The presence of TOBC

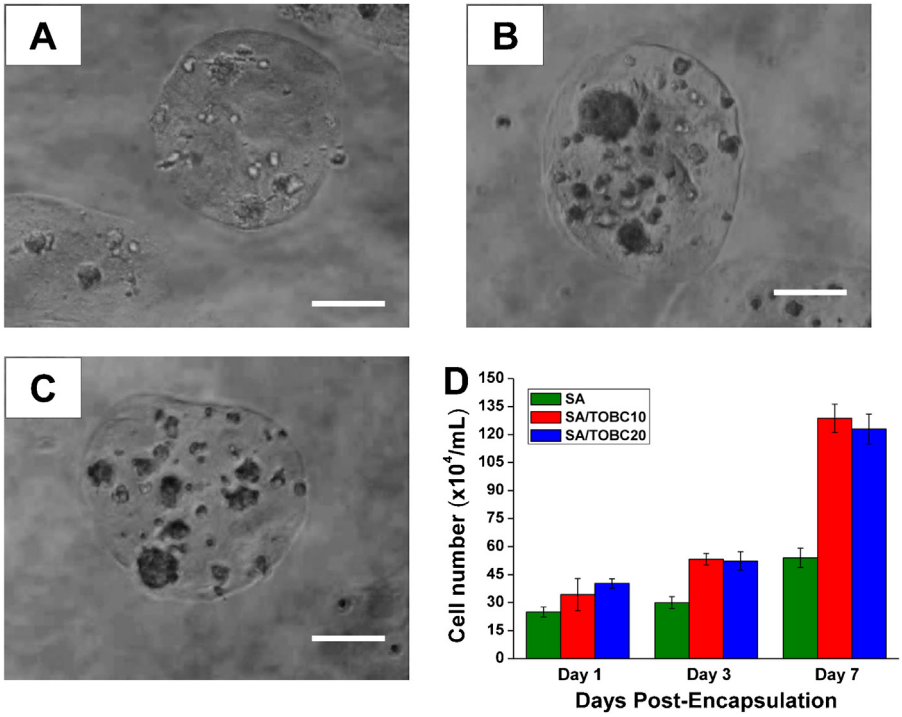

Fig. 7. Optical microscopy images of cells encapsulated in SA (A), SA/TOBC10 (B), and SA/TOBC20 (C). (D) Cell numbers for various SA/TOBC beads as function of cultured days. Scale bar = 250 μm.

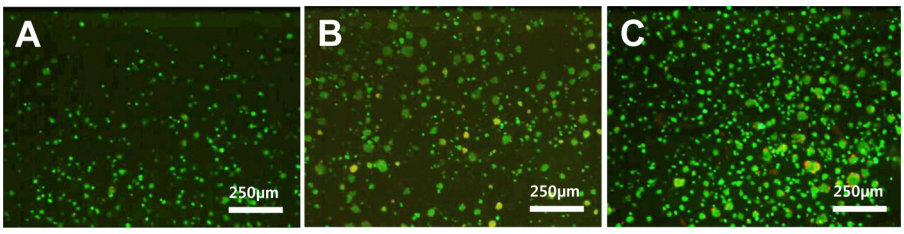

Fig. 8. Live/dead staining of cells recovered from beads. (A) SA, (B) SA/TOBC10 and (C) SA/TOBC20.

effectively protected the alginate beads from swelling and the loss of calcium ions due to the tightly packed nanofibrous structure (Fig. 5G).

The permeability of SA/TOBC beads was evaluated using 4 and 150 kDa FITC–dextran. The cross-sectional confocal images of the beads illustrated the permeability of the different molecular weight FITC–dextran materials. Although small molecules (4 kDa FITC–dextran) could penetrate the beads within 2 h, the large molecules (150 kDa FITC–dextran) could not penetrate the beads even after 24 h (Fig. 6). This semi-permeable property of SA/TOBC likely plays important role in protecting encapsulated cells from immune biomolecules, such as IgM (950 kDa) and IgG (150 kDa), while allowing oxygen and low molecular weight biological compounds that are necessary for the survival and function of a cell (Pedraz & Orive, 2010), such as glucose (180 D) and carbon dioxide (44 Da), as well as secretary proteins, such as insulin (6 kDa), to permeate

Fig. 7 shows the optical microscopy images of cells encapsulated in SA, SA/TOBC10, and SA/TOBC20 beads after the incubation for 5 days. The cells were well encapsulated in each bead and proliferated by forming cell clusters, as shown in the images. The cells from each bead were incubated for several days, collected at various time points and counted. The cells encapsulated in SA/TOBC10 and SA/TOBC20 proliferated more readily than cells in SA beads.

Live/dead staining experiments were conducted to investigate the viability of the cells encapsulated in beads.(Fig. 8) The cells recovered from the beads were still alive, and more cells were encapsulated in the beads containing TOBC nanofibers than in SA beads. The cells could be efficiently encapsulated within the SA/TOBC beads, retained a high level of cell viability and preserved their ability to proliferate. Normally, isolated single cells encapsulated in beads showed a lower cell viability than aggregated cells. Therefore, the formation 3D aggregated cells aided survival and proliferation because the nanofibrous structure of TOBC could improve the cell proliferation.

4. Conclusions

We attempted to design alginate–cellulose composites to encapsulate cells stably. TEMPO-mediated oxidized bacterial cellulose (TOBC) improved the mechanical and chemical stability of the SA beads. The incorporation of TOBC and SA was confirmed via the analysis of the chemical structure and crystallinity of the composite. The cells encapsulated in the beads tended to aggregate and form a cluster. Specifically, the cells encapsulated in the TOBC/SA beads were more viable and proliferated more readily than were the cells in the SA beads due to the 3D fibrous contribution of TOBC, which was similar to the extracellular matrix. TOBC/SA composite are a potential candidate for the encapsulation of cells, such as β-cells that form islets to activate the secretion of insulin.

Acknowledgments

This research was supported by the Basic Science Research Program through the National Research Foundation of Korea (NRF), funded by the Ministry of Science, ICT & Future Planning (Grant number 2013023612).

References

Bratlie, K. M., York, R. L., Invernale, M. A., Langer, R., & Anderson, D. G. (2012). Materials for diabetes therapeutics. *Advanced Healthcare Materials*, *1*(3), 267–284.

Chan, E. S., Wong, S. L., Lee, P. P., Lee, J. S., Ti, T. B., Zhang, Z. B., Poncelet, D., Ravindra, P., Phan, S. H., & Yim, Z. H. (2011). Effects of starch filler on the physical properties of lyophilized calcium-alginate beads and the viability of encapsulated cells. *Carbohydrate Polymers*, *83*(1), 225–232.

Cordoba, A. L., Deladino, L., & Martino, M. (2013). Effect of starch filler on calcium–alginate hydrogels loaded with yerba mate antioxidants. *Carbohydrate Polymers*, *95*(1), 315–323.

Dong, H., Snyder, J. F., Williams, K. S., & Andzelm, J. W. (2013). Cation-induced hydrogels of cellulose nanofibrils with tunable moduli. *Biomacromolecules*, *14*(9), 3338–3345.

Draget, K. I., Steinsvag, K., Onsoyen, E., & Smidsrod, O. (1998). Na- and K-alginate; effect on Ca^{2+}-gelation. *Carbohydrate Polymers*, *35*(1–2), 1–6.

Fujisawa, S., Okita, Y., Fukuzumi, H., Saito, T., & Isogai, A. (2011). Preparation and characterization of TEMPO-oxidized cellulose nanofibril films with free carboxyl groups. *Carbohydrate Polymers*, *84*(1), 579–583.

Hu, W. L., Chen, S. Y., Yang, Z. H., Liu, L. T., & Wang, H. P. (2011). Flexible electrically conductive nanocomposite membrane based on bacterial cellulose and polyaniline. *Journal of Physical Chemistry B*, *115*(26), 8453–8457.

Isogai, A., Saito, T., & Fukuzumi, H. (2011). TEMPO-oxidized cellulose nanofibers. *Nanoscale*, *3*(1), 71–85.

Klemm, D., Heublein, B., Fink, H. P., & Bohn, A. (2005). Cellulose: Fascinating biopolymer and sustainable raw material. *Angewandte Chemie International Edition*, *44*(22), 3358–3393.

Lin, N., Bruzzese, C., & Dufresne, A. (2012). TEMPO-oxidized nanocellulose participating as crosslinking aid for alginate-based sponges. *ACS Applied Materials & Interfaces*, *4*(9), 4948–4959.

Orive, G., Hernandez, R. M., Gascon, A. R., Calafiore, R., Chang, T. M., De Vos, P., Hortelano, G., Hunkeler, D., Lacik, I., Shapiro, A. M., & Pedraz, J. L. (2003). Cell encapsulation: Promise and progress. *Nature Medicine*, *9*(1), 104–107.

Orive, G., Tam, S. K., Pedraz, J. L., & Halle, J. P. (2006). Biocompatibility of alginate-poly-L-lysine microcapsules for cell therapy. *Biomaterials*, *27*(20), 3691–3700.

Park, M., Chang, H., Jeong, D. H., & Hyun, J. (2013). Spatial deformation of nanocellulose hydrogel enhances SERS. *Biochip Journal*, *7*(3), 234–241.

Park, M., Cheng, J., Choi, J., Kim, J., & Hyun, J. (2013). Electromagnetic nanocomposite of bacterial cellulose using magnetite nanoclusters and polyaniline. *Colloids and Surfaces B: Biointerfaces*, *102*, 238–242.

Pedraz, J. L., & Orive, G. (2010). *Therapeutic applications of cell microencapsulation*. New York, NY, Austin, TX: Springer Science + Business Media, Landes Bioscience.

Rokstad, A. M., Lacik, I., de Vos, P., & Strand, B. L. (2014). Advances in biocompatibility and physico-chemical characterization of microspheres for cell encapsulation. *Advanced Drug Delivery Reviews*, *67-68*, 113–130.

Saito, T. (2010). Structural analysis of TEMPO-oxidized cellulose nanofibers. *Sen-I Gakkaishi*, *66*(7), P240–P242.

Santagapita, P. R., Mazzobre, M. F., & Buera, M. D. (2012). Invertase stability in alginate beads: Effect of trehalose and chitosan inclusion and of drying methods. *Food Research International*, *47*(2), 321–330.

Schmidt, J. J., Rowley, J., & Kong, H. J. (2008). Hydrogels used for cell-based drug delivery. *Journal of Biomedical Materials Research, A*, *87A*(4), 1113–1122.

Tam, S. K., Dusseault, J., Bilodeau, S., Langlois, G., Halle, J. P., & Yahia, L. (2011). Factors influencing alginate gel biocompatibility. *Journal of Biomedical Materials Research, A*, *98A*(1), 40–52.

Watanabe, K., Tabuchi, M., Morinaga, Y., & Yoshinaga, F. (1998). Structural features and properties of bacterial cellulose produced in agitated culture. *Cellulose*, *5*(3), 187–200.

Zhang, T. J., Wang, W., Zhang, D. Y., Zhang, X. X., Ma, Y. R., Zhou, Y. L., & Qi, L. M. (2010). Biotemplated synthesis of gold nanoparticle-bacteria cellulose nanofiber nanocomposites and their application in biosensing. *Advanced Functional Materials*, *20*(7), 1152–1160.

Zhang, W. J., Zhao, S. T., Rao, W., Snyder, J., Choi, J. K., Wang, J. F., Khan, I. A., Saleh, N. B., Mohler, P. J., Yu, J. H., Hund, T. J., Tang, C. B., & He, X. M. (2013). A novel core–shell microcapsule for encapsulation and 3D culture of embryonic stem cells. *Journal of Materials Chemistry B*, *1*(7), 1002–1009.